Global Change Biology

WILEY

Global Change Biology

RESEARCH ARTICLE

Excessive Wetness Suppresses Carbon Sink of Amazon Forest Under Seasonal Water Surplus

Shulin Ren[1,2,3] | Xiyan Xu[1] | Gensuo Jia[1,2] | Paulo Artaxo[4,5] | Luiz A. T. Machado[5,6] | Juan A. G. Montes[7] | Carlos A. Nobre[8] | Luciana Rizzo[5] | Xiangming Xiao[9]

[1]State Key Laboratory of Earth System Numerical Modeling and Application, Institute of Atmospheric Physics, Chinese Academy of Sciences, Beijing, China | [2]University of Chinese Academy of Sciences, Beijing, China | [3]Shanxi Climate Center, Taiyuan, China | [4]Center for Sustainable Amazon Studies, University of São Paulo, São Paulo, Brazil | [5]Instituto de Física, University of São Paulo, São Paulo, Brazil | [6]Max Planck Institute for Chemistry, Mainz, Germany | [7]Universidad Nacional Pedro Ruiz Gallo, Lambayeque, Peru | [8]Institute of Advanced Studies, University of São Paulo, São Paulo, Brazil | [9]School of Biological Sciences, University of Oklahoma, Norman, Oklahoma, USA

Correspondence: Xiyan Xu (xiyan.xu@tea.ac.cn)

Received: 23 December 2024 | **Revised:** 1 July 2025 | **Accepted:** 14 July 2025

Funding: This work was supported by National Natural Science Foundation of China (NSFC#42261144754) and Fundação de Amparo à Pesquisa do Estado de São Paulo (FAPESP#2022/07974-0).

Keywords: Amazon forest | carbon sink | GPP | PAR | water surplus | wetness

ABSTRACT

The hydrological cycle in the Amazon basin has been shifted to a "wet season get wetter while dry season get drier" pattern. How the shifted hydrological pattern has been influencing the carbon budget of the Amazon forest remains unknown. Based on multiple observationbased carbon fluxes and climate datasets, we found that the carbon sink of the Amazon forest decreased over the past two decades, with 60.3% of the decreases occurring outside of the area of direct anthropogenic disturbances and approximately 52.6% of the decreases occurring in the wet season. The decreased carbon sink was dominated by the declined photosynthetic carbon uptake inferred by gross primary production (GPP). During the wet season, the entire Amazon basin is characterized by water surplus with climatically low photosynthetically active radiation (PAR), and the western to southern Amazon basin showed wetting trends with increased precipitation and decreased vapor pressure deficit (VPD), which enhanced the limitation of PAR, thereby reducing the GPP and thus the carbon sink. During the dry season, although the decreased GPP and carbon sink were mainly attributed to water stress associated with decreased precipitation and increased VPD, the excessive wetness with PAR limitation suppressed the GPP in the northwestern water surplus regions. We highlight the negative impacts of excessive seasonal wetness other than increased aridity on the carbon sink of the Amazon forest.

1 | Introduction

Forests in the Amazon basin store approximately 123 Pg of biomass carbon (Malhi et al. 2006) and act as a strong carbon sink (Brienen et al. 2015). However, recent studies suggested a carbon loss from the Amazon basin due to climate change and anthropogenic disturbances (Csillik et al. 2024; Pan et al. 2024). Severe drought leads to carbon loss and has a persistent impact on the carbon sink of the Amazon forest function (Yang et al. 2018). Deforestation and biomass burning cause carbon loss and even shift the forests from a carbon sink to a carbon source in the southeastern Amazon (Basso et al. 2023; Gatti et al. 2021). Forest fragmentation after deforestation exerts an edge effect, which leads to further carbon loss (Silva Junior et al. 2020).

The forest loss feedbacks to the climate system interacting with large-scale climate change, which has altered the regional climate in the Amazon basin. Increased seasonality characterized

by enhanced convective cloudiness in the wet season but less convection in the dry season was observed in deforested areas during the 1980s and 1990s (Durieux et al. 2003). During the dry season, forest loss even causes precipitation anomalies varying regionally. Khanna et al. (2017) revealed that in the State of Rondônia, Brazil, when the southeastern deforested areas became drier, the northwestern deforested areas became wetter. Besides, it is estimated that annual precipitation decreases with deforestation when forest loss exceeds approximately 23% at a large scale in the Brazilian Amazon (Leite-Filho et al. 2021). Deforestation reduces evapotranspiration, dries the lower atmosphere, and increases the air temperature in the dry season, which is more pronounced in the southeastern Amazon basin, where forest loss is the greatest (Alkama and Cescatti 2016; Xu et al. 2022). As temperature increases, atmospheric and soil aridity is intensified by accelerating water loss from soil and increasing atmospheric saturated vapor pressure (Hammond et al. 2022).

The rise of atmospheric aridity reduces stomatal conductance (McAdam and Brodribb 2015; Slot et al. 2024), thereby suppressing photosynthesis, especially in the dry season (Grossiord et al. 2020). The carbon uptake reductions by increased VPD partly offset the positive CO_2 fertilization effect under climate change (Yuan et al. 2019). Besides, high evaporative demand due to high VPD aggravates soil moisture extraction (Qing et al. 2022), which could induce hydraulic failure and then cause tree mortality (Rowland et al. 2015). During the strong drought in 2005, increased temperature and moisture stress caused more than 1.2 Pg C of biomass loss in the Amazon forest (Marengo et al. 2008; Phillips et al. 2009). By contrast, Green et al. (2020) found that increased VPD stimulated photosynthesis during both the dry and wet seasons, because low VPD may slow down carbon diffusion and promote the prevalence of phytopathogens, thereby inhibiting photosynthesis. It raises the question of whether the increased dryness can enhance the carbon sink in the Amazon basin.

Although the droughts have become more common in the dry season, the Amazon basin, specifically in climatologically wet regions, is recorded with increased precipitation in the wet season in recent decades (Chou et al. 2013; Wang et al. 2018). During the wet season, increased precipitation with concurrent cloudiness limits the solar radiation reaching the surface (Collow et al. 2016). Increased precipitation also hinders soil drainage in the regions with shallow water tables, enhancing flooding conditions and reducing oxygen concentration in the soil (Fan et al. 2017), which easily leads to tree mortality (Moser et al. 2019). Besides, high precipitation maintains a humid environment that increases the risk of fungal disease (Romero et al. 2022).

As climate warms, the warmer air can hold more water vapor in the wet regions (Wentz et al. 2007), and the convergence and ascending of air promote more precipitation formation (Chou et al. 2009), which may enhance the impacts of precipitation on forest carbon balance. Based on eddy covariance observations, Restrepo-Coupe et al. (2024) found that reduced radiation under positive precipitation anomalies resulted in a decline in the carbon sink of the Amazon tropical forest during the 2008 La Niña wet event. However, how the seasonal enhancement of wetness has been affecting the carbon sink of the Amazon forest remains unknown. In this study, we utilized multiple observation-based datasets to analyze the changes in the carbon sink of the Amazon basin in the wet and dry seasons during 2001–2018 and explored the influence of seasonal excessive wetness on the forest carbon uptake.

2 | Data and Methods

2.1 | Seasonal Water Availability in the Amazon Basin

The Amazon basin extends over more than one climate zone, and the allocation of annual and seasonal precipitation is distinguished in different climate zones (Beck et al. 2018). Thus, a differentiated definition of wet and dry seasons for different regions of the Amazon basin is necessary. For each grid, we defined the 6 months of a calendar year with the most precipitation as the wet season and the remaining 6 months with the least precipitation as the dry season. The 6 months within the year with most or least precipitation can be discontinuous or contiguous, which depends on the relative amount of monthly precipitation during the year. The monthly 0.05° Climate Hazards Center InfraRed Precipitation with Station data (CHIRPS) dataset (Funk et al. 2015) was first resampled to a 0.5° grid as the mean precipitation in 10×10, 0.05° grids. Then we used the regridded precipitation dataset to define the wet and dry seasons for each 0.5° grid and for each year over 2001–2018, which is the period when both climate and carbon flux datasets are available.

We calculated the 6-month accumulated water availability (WA) in the wet and dry seasons in the Amazon basin for each year over 2001–2018, which is expressed as:

$$\mathrm{WA} = P - \mathrm{ET} \tag{1}$$

$$\mathrm{ET} = E_b + E_i + E_t \tag{2}$$

where P is the 6-month total precipitation calculated with the resampled CHIRPS 0.5° precipitation, and ET is the 6-month total evapotranspiration in the wet and dry seasons. E_b is bare-soil evaporation, E_i is interception loss, and E_t is transpiration. The E_b, E_i, and E_t are from the 0.25° monthly Global Land Evaporation Amsterdam Model (GLEAM) (Martens et al. 2017; Miralles et al. 2011). The ET was resampled to 0.5° resolution as the mean ET in 2×2, 0.25° grids. Then, the average water availability in each grid during 2001–2018 was calculated for the wet and dry seasons. The areas with positive water availability ($\mathrm{WA} > 0$) are under water surplus, where the water supply is sufficient for vegetation (Seddon et al. 2016). The areas with negative water availability ($\mathrm{WA} < 0$) are considered under water deficit, where water supply from precipitation alone cannot meet the water demand of vegetation (Konapala et al. 2020).

2.2 | Excluding Areas With Direct Anthropogenic Disturbances

The Amazon basin is dominantly covered by evergreen broadleaf forest, that is, tropical rainforest, which has experienced

intense natural and direct anthropogenic disturbances in the past decades (Csillik et al. 2024). Here, we aim to identify regions dominated by natural processes and ignore direct anthropogenic disturbances. Deforestation, logging, and fires were considered direct anthropogenic disturbances because fires in this region are highly related to land use change activities (Ren et al. 2024). The Terra and Aqua combined Moderate Resolution Imaging Spectroradiometer (MODIS) Land Cover Type data product (MCD12Q1 Version 6.1) at 500-m resolution (Friedl and Sulla-Menashe 2022) was used to quantify the land use and land cover changes during 2001–2018. The land cover in 2001 was regarded as the initial land cover type. When the type in any given year after 2001 was different from that in 2001 in a 500-m grid, the land cover type was altered. The proportion of the total area of land cover changes (f_{LC}) over 18 years in each 0.5° grid was then calculated.

The fire disturbance was quantified with the Terra and Aqua combined MODIS burned area data product (MCD64A1 Version 6.1) at 500-m resolution (Giglio et al. 2021). Then, we summed the burned area and converted it to the proportion of burned area (f_{BA}) in each 0.5° grid during 2001–2018. In addition, the global forest change (GFC) dataset at 30-m resolution (Hansen et al. 2013) was used to identify the area of forest loss. We calculated the proportion of forest loss (f_{FL}) in each 0.5° grid over 18 years. To account for direct anthropogenic disturbances in the Amazon basin as much as possible, we selected the maximum one among the f_{LC}, f_{BA}, f_{FL} in each 0.5° grid, which was used to infer the area proportion of direct anthropogenic disturbances (f_D = maximum (f_{LC}, f_{BA}, f_{FL})). If f_D is larger than 5%, we considered the grid was affected by direct anthropogenic disturbances; otherwise, the grid was only affected by climate change.

2.3 | Carbon Fluxes of the Amazon Forest

The FLUXCOM (RS + METEO) initiative provides a collection of pre-2018 terrestrial carbon data products based on machine learning, which integrates FLUXNET site-level observations, satellite remote sensing, and meteorological data (Jung et al. 2020). It provides an opportunity to study carbon fluxes on a global scale, although sparse flux towers and humid micrometeorology may lead to uncertainties in tropical carbon fluxes estimation (Botía et al. 2022; Jung et al. 2020). We used FLUXCOM monthly net ecosystem exchange (NEE), terrestrial ecosystem respiration (TER), and gross primary production (GPP) products at 0.5° resolution to estimate their changes over 2001–2018. The net ecosystem productivity (NEP) was used as the carbon sink of the terrestrial ecosystem, which is expressed as:

$$\mathrm{NEP} = -\mathrm{NEE} = \mathrm{GPP} - \mathrm{TER} \quad (3)$$

In tropical forests, satellite observations are easily interrupted by excessive wetness and cloud cover, which affects the data quality. Therefore, in addition to the FLUXCOM GPP product, three other GPP products developed based on different algorithms were used. The 8-Day Terra MODIS GPP product at 500-m resolution (MOD17A2H Version 6.0) is based on the radiation-use efficiency concept (Running et al. 2015). The monthly GPP product developed with the Vegetation Photosynthesis Model (VPM) at 0.05° resolution is based on an improved light use efficiency model and employs a different treatment for C3 and C4 photosynthesis pathways (Zhang et al. 2017). The process-based Penman-Monteith-Leuning Evapotranspiration V2 (PML_V2) GPP product is at 500-m and 8-day resolution (Zhang et al. 2019). The PML GPP product treats carbon dioxide as an independent environmental constraint for carbon assimilation in the model to optimize GPP simulations. We integrated the 8-day MODIS and PML GPP into the monthly accumulated GPP. The three GPP products over 2001–2018 were resampled to 0.5° as the mean GPP within each 0.5° grid to accommodate the resolution and time span of FLUXCOM GPP, respectively.

We calculated the total NEP, TER, and GPP in the 6-month wet and dry seasons, respectively. Using the 6-month wet and dry season definition enables the calculation of annual cumulative NEP, TER, and GPP in two periods with the same duration. Then, the trends of NEP (T_{NEP}), TER (T_{TER}), and GPP (T_{GPP}) for each 0.5° grid from 2001 to 2018 were calculated with the Theil-Sen regression in the wet and dry seasons (Figures 1 and S1). The Theil-Sen trend analysis is a non-parametric statistical method for estimating trends in time series, and it can mitigate the influence of outliers on the trends (Donat et al. 2016). The statistical significance of trends was evaluated with 95% confidence via the Mann-Kendall test.

Considering spatial heterogeneities in precipitation seasonality, we also calculated NEP and precipitation trends in three consecutive months with the highest and lowest precipitation, which were used as optional definitions of wet and dry seasons, respectively, in the Amazon basin (Wang et al. 2024). The trends of seasonal NEP and precipitation were calculated using an additional definition of wet and dry seasons based on the relative magnitudes of monthly precipitation (P) and potential evapotranspiration (PET) (Guan et al. 2015). The PET is from Terra Moderate Resolution Imaging Spectroradiometer (MODIS) Net Evapotranspiration product (MOD16A2GF Version 6.1) (Running et al. 2017) with 500-m and 8-day resolution. The monthly accumulated PET was calculated and then resampled to a 0.5° resolution as the mean PET of all the 500 m grids within each 0.5° grid. The dry season is defined as the months when $P < \mathrm{PET}$, while the wet season is defined as the months when $P \geq \mathrm{PET}$.

As four GPP products were used in this study, we first evaluated the products in representing GPP trends across the Amazon basin. All four GPP products showed decreasing GPP trends in the western to southwestern Amazon basin during the wet season (Figure S1). Besides, three GPP products indicated increasing GPP trends in the northeastern and northwestern Amazon basin during the wet season, although differences in the magnitudes of the GPP trends of the four datasets exist (Figure S1). During the dry season, these datasets showed decreasing GPP trends in the southeastern Amazon basin except for MODIS GPP (Figure S1). The mean GPP trends of the four GPP products were then calculated to compromise uncertainties of each product. In addition, the grids were highlighted if three or more of the products showed the same sign of GPP trends.

To evaluate the relative contribution of GPP and TER to NEP changes during 2001–2018, the relative contribution of T_{TER} and T_{GPP} to the T_{NEP} was quantified following (Zhang et al. 2023) as

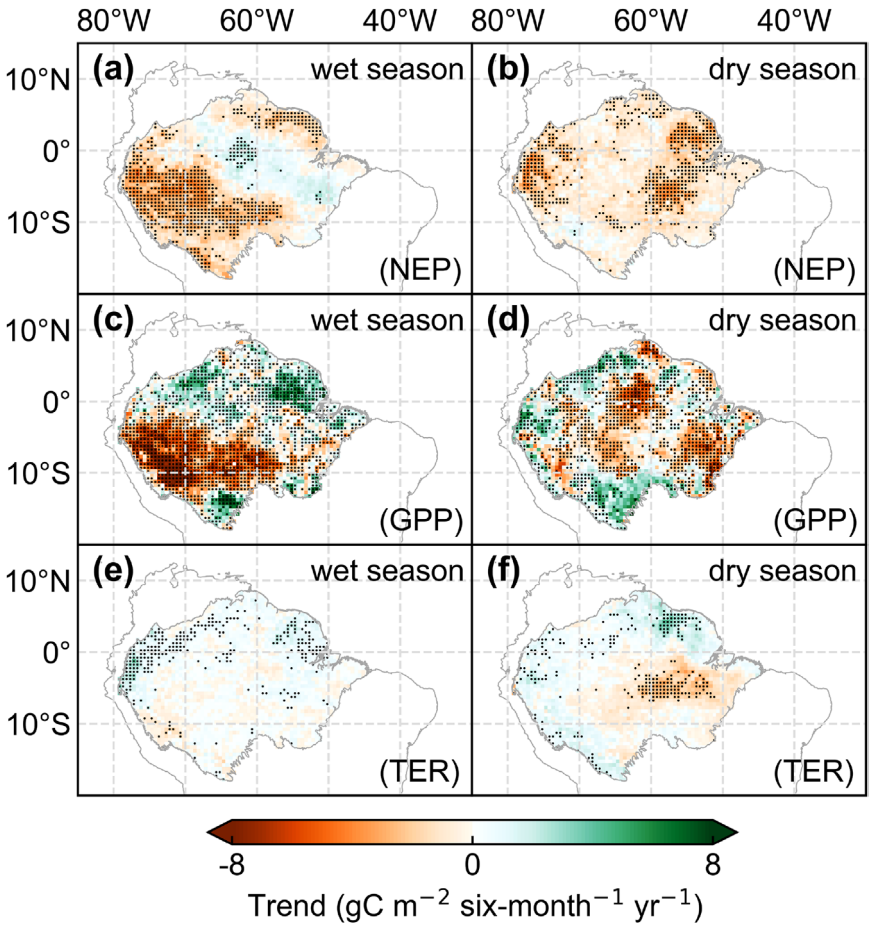

FIGURE 1 | Trends of carbon fluxes in the Amazon basin during 2001–2018. The trends in net ecosystem productivity (T_{NEP}) in (a) the wet season and (b) the dry season. The trends in gross primary production (T_{GPP}) in (c) the wet season and (d) the dry season. The trends in terrestrial ecosystem respiration (T_{TER}) in (e) the wet season and (f) the dry season. The statistically significant trends with 95% confidence in (a), (b), (e), and (f), and three or more of GPP products showed the same sign of T_{GPP} in (c) and (d) are shaded with black dots.

$$RC_X = \frac{|X|}{|X| + |Y|} \times 100\% \quad (4)$$

where RC_X is the relative contribution of X to T_{NEP}. When X is T_{TER}, Y is T_{GPP}, and vice versa. X dominates the T_{NEP} when $RCx > 60\%$; while Y dominates the T_{NEP} when $RCx < 40\%$; otherwise, X and Y play a comparable role in the T_{NEP}.

The Equation (4) was also used to quantify the relative contribution of seasonal T_{NEP} to the annual T_{NEP}, in which when X is the wet-season T_{NEP}, Y is the dry-season T_{NEP}, and vice versa. X dominates the annual T_{NEP} when $RCx > 60\%$, while Y dominates the annual T_{NEP} when $RCx < 40\%$; otherwise, X and Y play comparable roles in the annual T_{NEP}. Similarly, we estimated the relative contribution of seasonal T_{GPP} to the annual T_{GPP}.

2.4 | Climate Impact on Carbon Fluxes of the Amazon Forest

Four climate variables were used to evaluate the change of climate pattern and its impact on carbon fluxes of the Amazon forest. Monthly mean photosynthetically active radiation (PAR) is the sum of all-sky surface PAR direct flux and all-sky surface PAR diffuse flux, both of which were from the Clouds and the Earth's Radiant Energy System (CERES) synoptic 1° (SYN1deg) Edition 4.1 product (Wielicki et al. 1996). Monthly total precipitation was analyzed with the CHIRPS dataset. The monthly mean 2-m air temperature (T) was analyzed with the 0.1° European Centre for Medium-Range Weather Forecasts (ECMWF) ERA5-Land monthly reanalysis dataset (Muñoz Sabater 2019). The monthly mean VPD was calculated according to Equation (5) (Barkhordarian et al. 2019):

$$VPD = c_1 \times e^{\left(\frac{c_2 \times T}{c_3 + T}\right)} - c_1 \times e^{\left(\frac{c_2 \times T_d}{c_3 + T_d}\right)} \quad (5)$$

where $c_1 = 6.11$ hPa, $c_2 = 17.5$, $c_3 = 240.978$°C. The T_d is the 2-m dew point temperature from the ERA5-Land monthly reanalysis dataset.

The precipitation, PAR, temperature, and VPD were averaged within 0.5° resolution, respectively, to accommodate the resolution of GPP. Moreover, we calculated the total precipitation and the mean PAR, temperature, and VPD in the wet and dry seasons. Then, the trends of precipitation, PAR, temperature, and VPD during 2001–2018 were calculated with the Theil-Sen regression in the wet and dry seasons. Mann-Kendall test with 95% confidence was applied to evaluate the statistical significance of trends.

To assess the impact of climate variables on GPP, the relationship between detrended GPP and each detrended climate variable was evaluated via Pearson's correlation analysis. We also applied Pearson's correlation analysis to analyze the relationship between precipitation and PAR. The statistical significance of correlations was assessed by student's test with 95% confidence.

3 | Results

3.1 | Dominated Carbon Sink Decline in the Wet Season

Amazon forest exhibits a carbon sink with a strong capacity in the north and west of the Amazon basin during 2001–2018, according to the FLUXCOM dataset (Figure S2). However, the carbon sink decreased ($T_{NEP}<0$) by about 15.6 TgC yr^{-2} from 2001 to 2018. The decrease in carbon sink is higher in the 6-month relatively wet season (about 8.2 TgC 6-month^{-1}yr^{-1}) than in the 6-month relatively dry season (about 7.4 TgC 6-month^{-1}yr^{-1}). The carbon sink decline was more intense in the wet season than that in the dry season, mainly in the western and southern Amazon basin, although the carbon sink reduction in the dry season was more widespread (Figures 1 and S3). The seasonal contrast changes in carbon sink were demonstrated in the wet and dry seasons defined with three consecutive months with the highest and lowest precipitation, respectively, and in the wet and dry seasons defined with the relative magnitudes of monthly precipitation and potential evapotranspiration (Figure S4a,b,e,f). The dominated carbon sink decline in the wet season is consistent with a significant decrease in GPP in the western to southern Amazon basin as the basin-wide TER trends were low and insignificant (Figure 1c,e). Multiple GPP products demonstrate the significant decline in GPP in the western and southern Amazon basin (Figure S1). As a result, the GPP contributes 82.5% to the trends of NEP in the wet season (Figures 2d and S3c). By contrast, the GPP contributes 67.8% to the trends of NEP in the dry season (Figures 2d and S3d).

To distinguish the major driver of the NEP and GPP declines, the Amazon basin with anthropogenic disturbances ($f_D>5\%$) and without anthropogenic disturbances ($f_D\leq5\%$) during 2001–2018 was identified (Figure 2a). The area with anthropogenic disturbances and without anthropogenic disturbances accounts for about 46% and 54% of the Amazon basin, respectively (Figure 2b). In the wet season, most of the NEP and GPP declines were outside the regions of direct anthropogenic

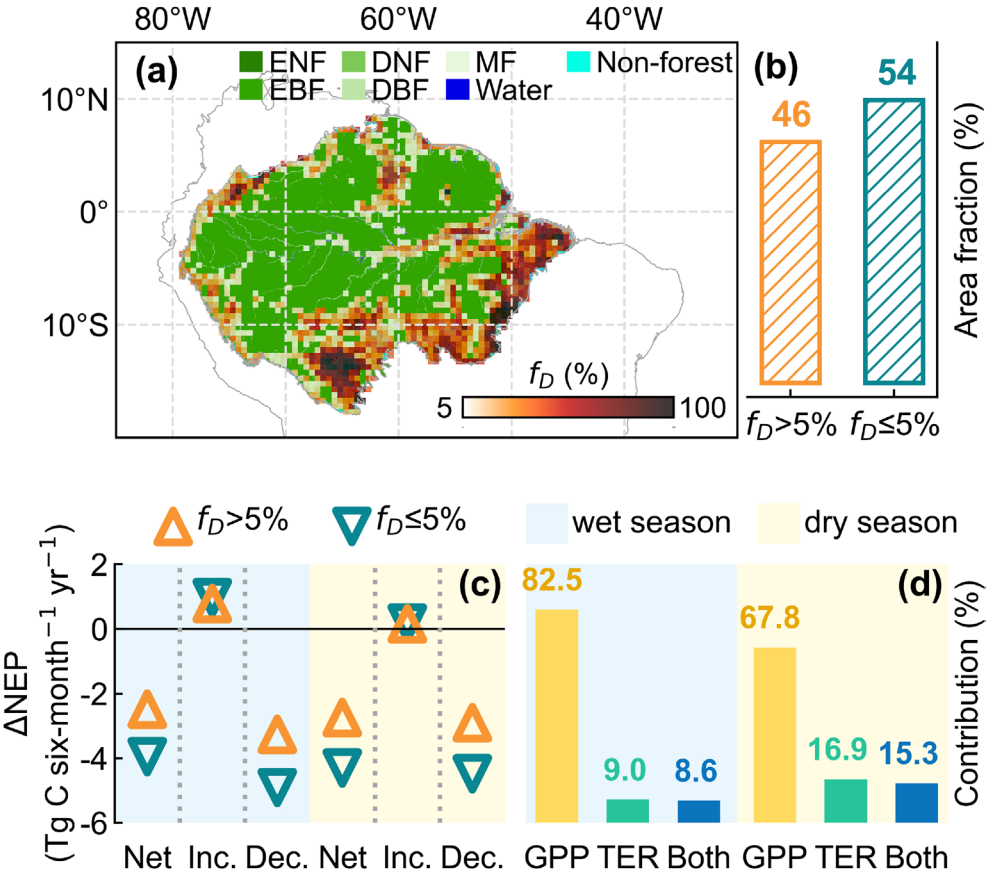

FIGURE 2 | The regional and seasonal differences in carbon sink changes in the Amazon basin during 2001–2018. The distribution of land cover types in 2001 and a fraction of direct anthropogenic disturbances (f_D) during 2001–2018 are shown in (a). Non-forest in (a) is an aggregation of shrublands, savannas, grasslands, croplands, permanent wetlands, urban and built-up lands, permanent snow and ice, and barren according to the International Geosphere-Biosphere Programme (IGBP) classification. The proportion of area with direct anthropogenic disturbances ($f_D>5\%$) and without direct anthropogenic disturbances ($f_D\leq5\%$) in the Amazon basin are shown in (b). (c) the total T_{NEP} in the areas with direct anthropogenic disturbances and without direct anthropogenic disturbances in the wet and dry seasons, respectively. The Inc., Dec., and Net in (c) represent $T_{NEP}>0$, $T_{NEP}<0$, and the net T_{NEP} of the whole Amazon basin, respectively. (d) the relative contribution of T_{TER} and T_{GPP} to the T_{NEP} in the wet and dry seasons over the Amazon basin during 2001–2018. "both" in (d) indicates that T_{TER} and T_{GPP} play a comparable role in the T_{NEP}.

disturbances (Figures 1 and 2a). The wet-season carbon sink reduction in the areas without direct anthropogenic disturbances was about 1.4 gC m^{-2} 6-month^{-1} yr^{-1}(about 4.9 TgC 6-month^{-1} yr^{-1} in all the areas with $f_D \leq 5\%$), while the reduction of carbon sink in the area with anthropogenic disturbances was about 1.0 gC m^{-2} 6-month^{-1} yr^{-1} (about 3.3 TgC 6-month^{-1} yr^{-1} in all the areas with $f_D > 5\%$) (Figure 2c). The net reduction of carbon sink in the wet season was slightly lower than that in the dry season because the enhanced carbon sink in the central and eastern Amazon basin partially offset the declined carbon sink in the southern and western Amazon basin during the wet season. However, the absolute reduction of carbon sink in the wet season was still greater than that in the dry season. The dry-season carbon sink reductions in the areas without and with direct anthropogenic disturbances were 1.3 gC m^{-2} 6-month^{-1} yr^{-1} (4.5 TgC 6-month^{-1} yr^{-1} in all the areas with $f_D \leq 5\%$) and 0.9 gC m^{-2} 6-month^{-1} yr^{-1} (2.9 TgC 6-month^{-1} yr^{-1} in all the areas with $f_D > 5\%$), respectively (Figure 2c).

3.2 | Changes in Seasonal Wetness in the Amazon Basin

The Amazon basin is humid, with total seasonal precipitation of more than 1000 mm and mean VPD below 6 hPa in more than 98% of the area during the wet season (Figure S5). Due to the high precipitation, the entire Amazon basin showed water surplus (WA > 0), especially in the western and northwestern Amazon basin in the wet season (Figure 3a). By contrast, except in the northwestern Amazon basin, the dry season was characterized by relatively higher temperatures and lower precipitation, which resulted in a water deficit (WA < 0) (Figures 3b and S5). During 2001–2018, the precipitation showed overall increasing trends, with more intensive increases in the western Amazon basin during the 6-month relatively wet season, the wettest consecutive 3 months, and the period when $P \geq$ PET (Figures 3e and S4c,g). Meanwhile, the VPD showed decreasing trends mainly in the western and southern Amazon basin (Figure 3c). As a result, the western to southern Amazon basin, which is climatically humid, became even wetter in the past two decades during the wet season. In contrast, the VPD increased extensively in the dry season (about 84.5% of the Amazon basin area), reinforcing atmospheric aridity in the water deficit regions (Figure 3d).

During the wet season, the decreased VPD in the western and southern Amazon basin over 2001–2018 can be explained by the increasing trends of precipitation with relatively stable temperatures (Figure S6). Due to the impact of excessive wetness, which is related to increased cloud cover and radiation hampering, the PAR decreased during the wet season (Figure S7), which aggravated the PAR limitation, especially in the western to southern Amazon basin where the PAR is climatically low due to high precipitation and humidity (Figure S5g). In the dry season, the increased VPD was dominantly driven by the significantly

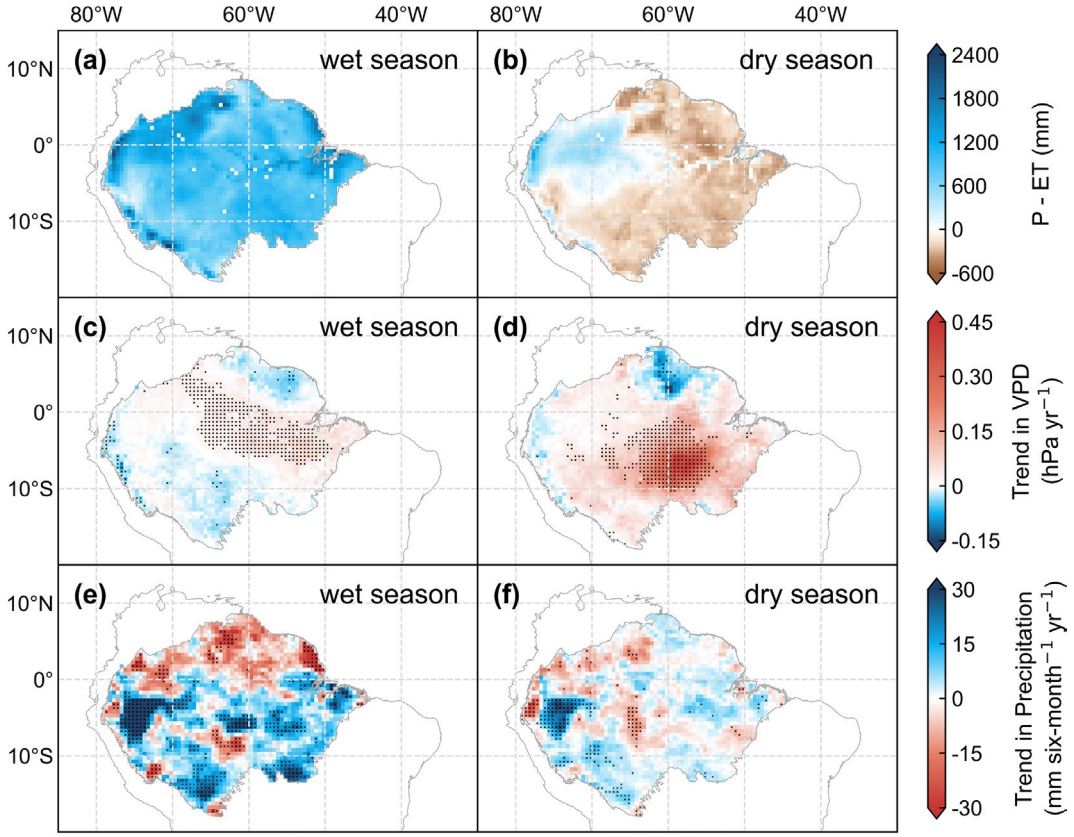

FIGURE 3 | Mean seasonal water availability and trends of precipitation and vapor pressure deficit (VPD) in the Amazon basin during 2001–2018. The mean water availability in (a) the wet season and (b) the dry season. Water availability is from precipitation (P) minus evapotranspiration (ET). The trends in VPD in (c) the wet season and (d) the dry season, and the trends in precipitation in (e) the wet season and (f) the dry season. The statistically significant trends with 95% confidence in (c–f) are shaded with black dots.

increasing trends of temperature, especially in the central and southeastern Amazon basin.

3.3 | Response of Photosynthetic Carbon Uptake to Seasonal Wetness Change

In the wet season, the entire Amazon basin showed enhanced PAR limitation due to increased precipitation under the seasonal water surplus (Figures S5 and S7). The GPP decreases with the decrease in PAR (r (GPP, PAR) > 0) (Figure S8a) and with the increase of precipitation (r (GPP, P) < 0) (Figure 4a). The GPP also decreases when VPD decreases (r (GPP, VPD) > 0) in almost all the Amazon basin (Figure 4b). Therefore, as the temperature changed at a relatively low rate and the PAR was hindered by increased cloudiness associated with increased precipitation (Figures S6a and S7a), the greater reduction in PAR contributed to the greater decline in GPP during 2001–2018 (Figure 5b).

During the dry season, only the northwestern Amazon basin showed water surplus (Figure 3b). In the water surplus regions, the GPP decreases when precipitation increases, and VPD decreases like that in the wet season (Figure 4d,e), which is demonstrated by the dominant negative correlation between GPP and precipitation and the positive correlation between GPP and VPD (Figure 4g,h). The decreased PAR with increased wetness contributed to the reduction of GPP in the water surplus regions (Figure 5d), where the GPP showed overall decreases with the decreased PAR (r (GPP, PAR) > 0, Figure S8c,e).

In the dry season, the majority of the area of the Amazon basin showed water deficit (Figure 3b), and the dominant GPP declined in the water deficit regions between 2001 and 2018 (Figure 5c,d). In the water deficit regions, GPP decreases with decreased precipitation (r (GPP, P) > 0), and water availability (r (GPP, WA) > 0), and the increase of VPD (r (GPP, VPD) < 0) (Figure 4d–i). The above results indicate that increased wetness in the water surplus regions suppresses photosynthesis no matter in the wet or dry seasons, while the increased wetness in the water deficit regions can mitigate water stress and thus be conducive to photosynthetic carbon uptake (Figure 6).

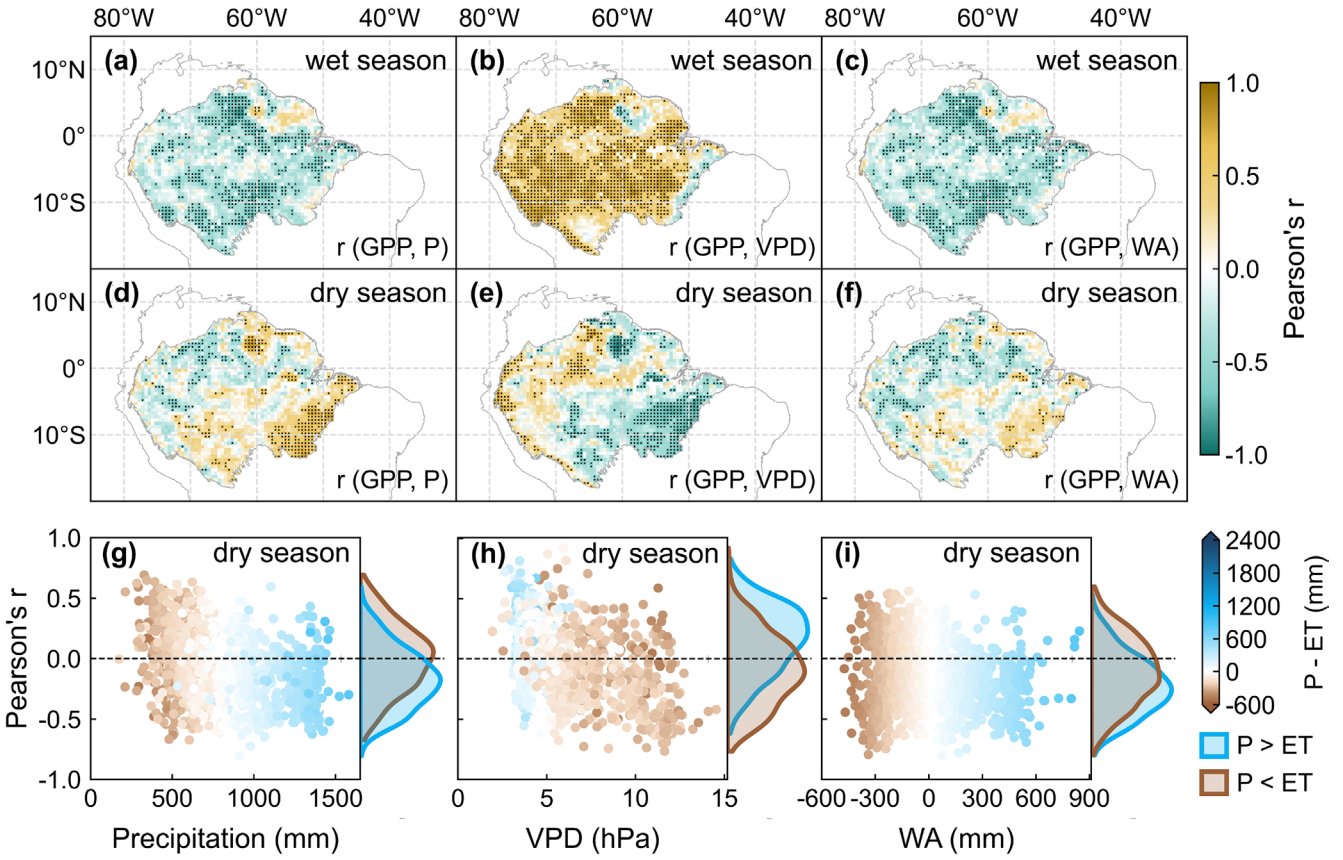

FIGURE 4 | Correlations between gross primary production (GPP) and precipitation (P), vapor pressure deficit (VPD) and water availability (WA) in the Amazon basin during 2001–2018. The distribution of Pearson's correlation between GPP and precipitation in (a) the wet season and (d) the dry season. The distribution of Pearson's correlation between GPP and VPD in (b) the wet season and (e) the dry season. The distribution of Pearson's correlation between GPP and WA in (c) the wet season and (f) the dry season. The statistically significant correlations with 95% confidence in (a–f) are shaded with black dots. The correlations between (g) GPP and precipitation, between (h) GPP and VPD and between (i) GPP and WA at different water availability levels during the dry season only, because water availability during the wet season is always positive with negative correlations between GPP and precipitation in (a) and between GPP and WA in (c) and with positive correlations between GPP and VPD in (b). The scatters in (g–i) correspond to the grids with $f_D \leq 5\%$ in the Amazon basin. The curves on the right side of (g–i) are the probability distribution functions of the scatters.

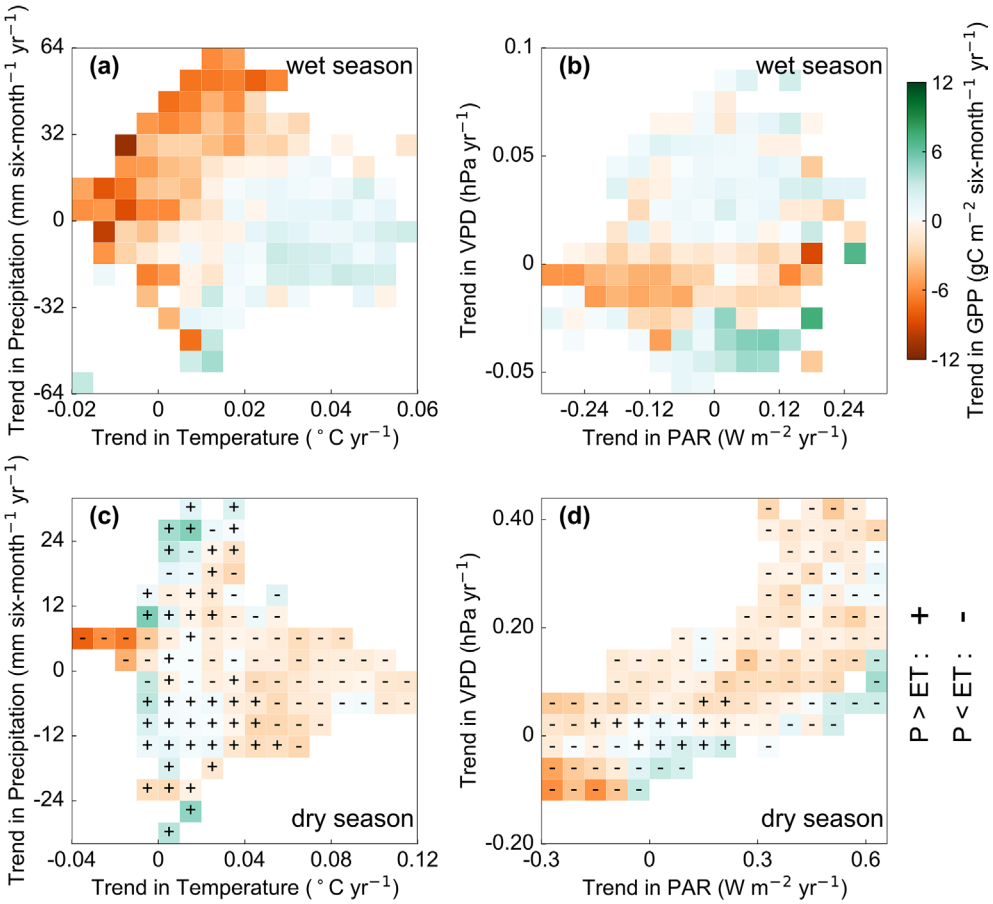

FIGURE 5 | Trends of GPP against trends of climate factors. The trends in GPP against the trends in precipitation and temperature in (a) the wet season and (c) the dry season. The trends in GPP against the trends in photosynthetically active radiation (PAR) and vapor pressure deficit (VPD) in (b) the wet season and (d) the dry season. In (a–d), the GPP in each cell is an average of GPP from all grids within the corresponding bin of climatological factors. Only the grids with $f_D \leq 5\%$ in the Amazon basin are considered in (a–d). In (c) and (d), the plus signs indicate water surplus ($P > \mathrm{ET}$) and the minus signs indicate water deficit ($P < \mathrm{ET}$).

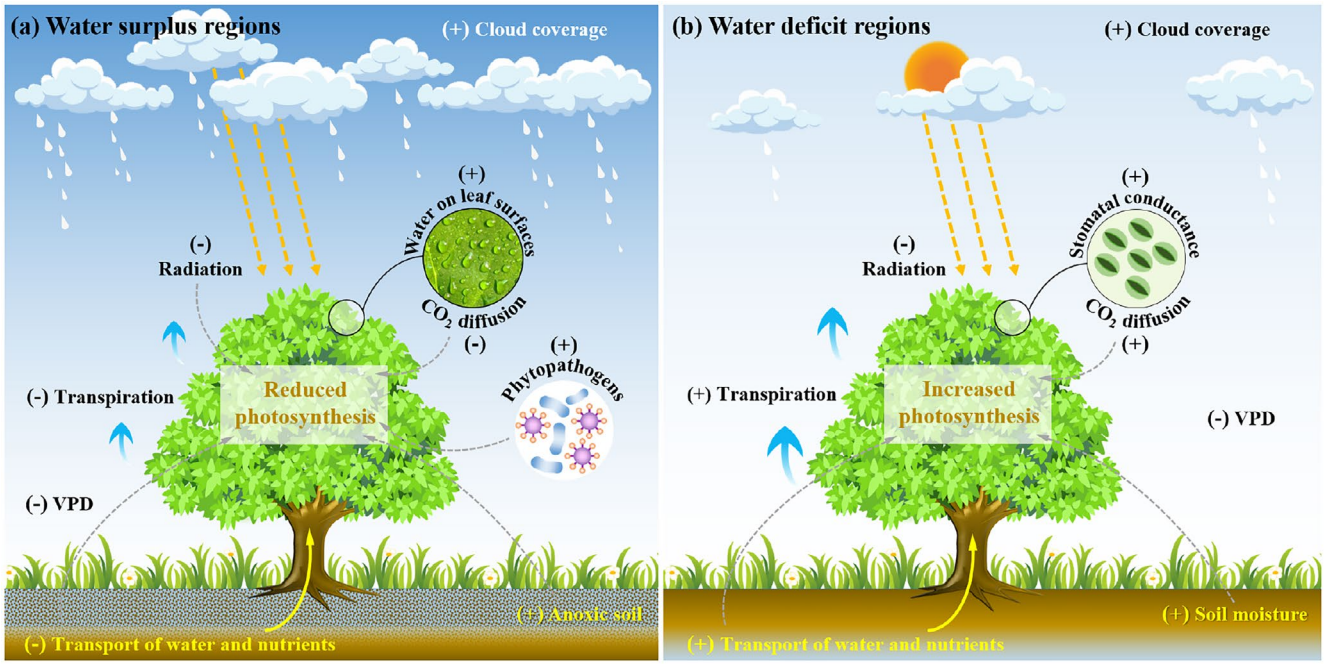

FIGURE 6 | Schematic diagram showing effects of excessive wetness on photosynthesis of the Amazon forest under (a) water surplus and (b) water deficit. The (+) and (–) denote the positive and negative effects of excessive wetness on processes linking to photosynthesis, respectively.

4 | Discussion and Conclusion

Amazon forest holds approximately 17% of the global vegetation carbon stocks (Fauset et al. 2015) and is a net carbon sink (Brienen et al. 2015). Our study revealed a reduction of carbon sink in the Amazon basin since the beginning of the 21st century, and more than half of the decreases occurred in the wet season. During the wet season, the declined GPP contributes about 82.5% to the trends of carbon sink reduction in the wet season, and the dominated carbon sink decline is consistent with GPP reduction in the western to southern Amazon basin.

We demonstrated that excessive wetness is one of the key factors causing the decline of GPP in the wet season (Figure 6a). The entire Amazon basin is characterized by a water surplus with an abundant supply of precipitation in the wet season. As precipitation further increases, excessive wetness with increasing cloud coverage can decrease incoming radiation and thus hinder photosynthesis (Green et al. 2020), which is demonstrated by the negative correlation between precipitation and PAR (Figure S7). Furthermore, a more humid environment in tropical forests is favorable for phytopathogen growth and dispersal, which may increase the risk of diseases for trees and their susceptibility to disturbances (McDowell et al. 2018; Swinfield et al. 2012); yet, the evidence to date is limited. The diseased trees are more likely to die off when wind storms concur with heavy precipitation during wet months (Aleixo et al. 2019). Besides, the increased frequency of storms with lightning in the wet season becomes a critical agent of mortality for some tropical tree species under climate change (Richards et al. 2022; Yanoviak et al. 2020).

The wetting trends in the wet season are consistent with decreased VPD in the majority area in the Amazon basin. We found extensive positive sensitivities of GPP to VPD in the water surplus regions where the VPD is below around 6 hPa in both the wet and dry seasons (Figures 4b,e,h and S5c,d). The low VPD can reduce the rate at which water is transferred from plants to the atmosphere and thus weaken transpiration, which is a driver for roots absorbing nutrients and water from the soil (Cernusak et al. 2011; Fricke 2017). Furthermore, extremely low VPD means that the moisture has a high potential to condense on leaves, which extends the duration of leaf wetness and facilitates phytopathogen establishment on the surface of leaves (Dawson and Goldsmith 2018). On the contrary, a drier environment created by higher VPD in the water surplus regions reduces the prevalence of phytopathogens and has beneficial influences on the photosynthetic efficiency of the leaves (Green et al. 2020).

In the dry season, we found positive correlations between PAR and precipitation mainly occurring in the Southern Hemisphere (Figure S7d), which might be related to the aerosol concentration induced by biomass-burning emissions. Aerosols reduce PAR via absorption and scattering (Malavelle et al. 2019); however, the wet deposition from precipitation enhances the aerosol removal (Ryu and Min 2022) and thus promotes the increase in PAR. Despite the increase of PAR, decreased GPP and water deficit are widespread in the Amazon basin during the dry season (Figure 5d).

In the dry season, sufficient water supply is a prerequisite for positive responses of photosynthesis to PAR increase (Chen et al. 2022; Guan et al. 2015). In the water deficit regions during the dry season, vegetation obtains water from subsurface water storage in addition to precipitation to meet the water requirements for growth (Guan et al. 2015). However, less precipitation and subsurface water supply may not be enough to meet the dry-season total water requirements of vegetation (Guan et al. 2015; Lian et al. 2024). Meanwhile, plants close their stomata to avoid excess water dissipation under high VPD; but this strategy can also cause tissue-level carbohydrate starvation and reduce growth (Grossiord et al. 2020). Under water stress, high evaporative demand is more likely to fill xylem conduits and rhizosphere with air, which inhibits the water flow, dries out tissues, and causes plant death (McDowell et al. 2008). Therefore, the inhibition of water stress to photosynthesis exceeds the stimulating impact of increased PAR in the water deficit regions, which is also demonstrated by ground-based observation that water stress induces the decrease of photosynthesis at water-limited sites in the dry season (Restrepo-Coupe et al. 2013). In addition, in the dry season under water limitation, plants preferentially allocate the accessible water to the growth of new leaves instead of carbon uptake, which hampers the photosynthetic carbon assimilation (Lian et al. 2024).

We defined water surplus and water deficit regions based on water availability calculated with precipitation and evapotranspiration. However, water availability to plants is also modulated by soil water supply, which mainly depends on the root depth, water table depth, and soil texture (Costa et al. 2023; Stocker et al. 2023). In some areas with deep water tables, forests are more likely to be in an environment with limited water access during the dry season because of less precipitation and deeper water tables being departed from roots (Barros et al. 2019; Costa et al. 2023). Furthermore, soil texture influences the water availability to plants by regulating the downward infiltration and the upward capillary rise (Fan et al. 2017). Generally, clay-dominated soils exhibit lower drainage capacity but stronger capacity for capillary rise compared to sandy soils (Miguez-Macho and Fan 2012). The soil texture and soil water content determine soil's nutrient storage capacity, which influences the hydraulic trade-off of plants. For example, plants growing in nutrient-rich soils prioritize rapid growth over embolism resistance and thus tend to have low water transport capacity under water stress (Oliveira et al. 2021). About 50% of the Amazon basin has shallow water table depths within five meters during the wet season (Costa et al. 2023), and the increased precipitation contributes additional water supply to the soils, which maintains water surplus conditions for plants. During the dry season, the eastern and northeastern Amazon basin has deep water table depths due to low precipitation, which may increase the difficulty for roots to access water (Costa et al. 2023; Yang et al. 2016). In addition, the soil texture mainly composed of loamy and sandy soils in these areas (Pavão et al. 2024) promotes water loss and thus restrains water availability for plants.

In this study, we analyzed the changes of carbon sink over the Amazon basin during 2001–2018. We found a decreasing trend in carbon sink of the Amazon forest even without direct anthropogenic disturbance, which is mainly caused by the GPP decline in the wet season when the entire Amazon basin is under water surplus.

Furthermore, the carbon sink decline in the wet season was more intense in the climatically humid western and southern Amazon basin, where precipitation has increased, and VPD has decreased in the past two decades, which demonstrates that excessive wetness with the limitation of photosynthetically active radiation suppressed the GPP and thus the carbon sink. The excessive wetness also suppressed the GPP during the dry season in the northwestern Amazon basin under water surplus. However, the decreased GPP and carbon sink in the water deficit regions during the dry season is attributed to water stress aggravated by decreased precipitation and increased VPD. Our study highlights the necessity of considering the negative impacts of excessive wetness on carbon sinks, particularly under the "wet season get wetter" hydrological cycle pattern due to anthropogenic and natural disturbances.

Author Contributions

Shulin Ren: formal analysis, investigation, software, visualization, writing – original draft. **Xiyan Xu:** conceptualization, funding acquisition, project administration, supervision, writing – original draft, writing – review and editing. **Gensuo Jia:** conceptualization, project administration, supervision, writing – original draft, writing – review and editing. **Paulo Artaxo:** supervision, writing – review and editing. **Luiz A. T. Machado:** funding acquisition, supervision, writing – review and editing. **Juan A. G. Montes:** supervision, writing – review and editing. **Carlos A. Nobre:** supervision, writing – review and editing. **Luciana Rizzo:** supervision, writing – review and editing. **Xiangming Xiao:** supervision, writing – review and editing.

Acknowledgments

This study is jointly funded by the Natural Science Foundation of China (NSFC#42261144754) and Fundação de Amparo à Pesquisa do Estado de São Paulo (FAPESP#2022/07974-0) under the Sustainable Development International Cooperation Program (SDIC).

Conflicts of Interest

The authors declare no conflicts of interest.

Data Availability Statement

The data that support the findings of this study are openly available in Zenodo at https://doi.org/10.5281/zenodo.16640042. The Climate Hazards Center InfraRed Precipitation with Station data (CHIRPS Version 2.0) were obtained from the Climate Hazards Center data server at https://data.chc.ucsb.edu/products/. The evapotranspiration data were obtained from Global Land Evaporation Amsterdam Model (GLEAM Version 3.8a) at https://www.gleam.eu. The MODIS/Terra+Aqua Land Cover Type data (MCD12Q1 Version 6.1) can be accessed from NASA LP DAAC at the USGS EROS Center at https://doi.org/10.5067/MODIS/MCD12Q1.061 and Google Earth Engine at https://developers.google.com/earth-engine/datasets/catalog/MODIS_061_MCD12Q1#description. The MODIS/Terra+Aqua Burned Area data (MCD64A1 Version 6.1) can be accessed from NASA LP DAAC at the USGS EROS Center at https://doi.org/10.5067/MODIS/MCD64A1.061 and Google Earth Engine at https://developers.google.com/earth-engine/datasets/catalog/MODIS_061_MCD64A1#dois. The Global Forest Change data in Version 1.11 were obtained from the University of Maryland (UMD) at https://glad.earthengine.app/view/global-forest-change. The FLUXCOM carbon fluxes were obtained from Data Portal of the Max Planck Institute for Biogeochemistry at https://www.bgc-jena.mpg.de/geodb/projects/Data.php. The MODIS/Terra Gross Primary Productivity data (MOD17A2H Version 6.0) can be accessed from NASA LP DAAC at the USGS EROS Center at https://doi.org/10.5067/MODIS/MOD17A2H.006. The VPM GPP product is openly available in Figshare at https://doi.org/10.6084/m9.figshare.c.3789814.v1. The PML GPP product in Version 2.0 was obtained from National Tibetan Plateau Data Center at https://doi.org/10.11888/Geogra.tpdc.270251 and Google Earth Engine at https://developers.google.com/earth-engine/datasets/catalog/CAS_IGSNRR_PML_V2_v018#description. The potential evapotranspiration data from MODIS/Terra Net Evapotranspiration product (MOD16A2GF Version 6.1) can be accessed from NASA LP DAAC at the USGS EROS Center at https://doi.org/10.5067/MODIS/MOD16A2GF.061 and Google Earth Engine at https://developers.google.com/earth-engine/datasets/catalog/MODIS_061_MOD16A2GF#dois. The CERES PAR data in Edition 4.1 were obtained from Atmospheric Science Data Center (ASDC) at https://doi.org/10.5067/TERRA+AQUA/CERES/SYN1DEGMONTH_L3.004A. The ERA5-Land reanalysis data were obtained from the Copernicus Climate Change Service (C3S) Climate Data Store (CDS) at https://doi.org/10.24381/cds.68d2bb30.

References

Aleixo, I., D. Norris, L. Hemerik, et al. 2019. "Amazonian Rainforest Tree Mortality Driven by Climate and Functional Traits." *Nature Climate Change* 9: 384–388. https://doi.org/10.1038/s41558-019-0458-0.

Alkama, R., and A. Cescatti. 2016. "Biophysical Climate Impacts of Recent Changes in Global Forest Cover." *Science* 351, no. 6273: 600–604. https://doi.org/10.1126/science.aac8083.

Barkhordarian, A., S. S. Saatchi, A. Behrangi, P. C. Loikith, and C. R. Mechoso. 2019. "A Recent Systematic Increase in Vapor Pressure Deficit Over Tropical South America." *Scientific Reports* 9, no. 1: 15331. https://doi.org/10.1038/s41598-019-51857-8.

Barros, F. d. V., P. R. L. Bittencourt, M. Brum, et al. 2019. "Hydraulic Traits Explain Differential Responses of Amazonian Forests to the 2015 El Niño-Induced Drought." *New Phytologist* 223: 1253–1266. https://doi.org/10.1111/nph.15909.

Basso, L. S., C. Wilson, M. P. Chipperfield, et al. 2023. "Atmospheric CO_2 Inversion Reveals the Amazon as a Minor Carbon Source Caused by Fire Emissions, With Forest Uptake Offsetting About Half of These Emissions." *Atmospheric Chemistry and Physics* 23, no. 17: 9685–9723. https://doi.org/10.5194/acp-23-9685-2023.

Beck, H. E., N. E. Zimmermann, T. R. McVicar, N. Vergopolan, A. Berg, and E. F. Wood. 2018. "Present and Future Köppen-Geiger Climate Classification Maps at 1-km Resolution." *Scientific Data* 5, no. 1: 180214. https://doi.org/10.1038/sdata.2018.214.

Botía, S., S. Komiya, J. Marshall, et al. 2022. "The CO_2 Record at the Amazon Tall Tower Observatory: A New Opportunity to Study Processes on Seasonal and Inter-Annual Scales." *Global Change Biology* 28: 588–611. https://doi.org/10.1111/gcb.15905.

Brienen, R. J. W., O. L. Phillips, T. R. Feldpausch, et al. 2015. "Long-Term Decline of the Amazon Carbon Sink." *Nature* 519, no. 7543: 344–348. https://doi.org/10.1038/nature14283.

Cernusak, L. A., K. Winter, and B. L. Turner. 2011. "Transpiration Modulates Phosphorus Acquisition in Tropical Tree Seedlings." *Tree Physiology* 31, no. 8: 878–885. https://doi.org/10.1093/treephys/tpr077.

Chen, R., L. Liu, and X. Liu. 2022. "The Negative Impact of Excessive Moisture Contributes to the Seasonal Dynamics of Photosynthesis in Amazon Moist Forests." *Earth's Future* 10, no. 1: e2021EF002306. https://doi.org/10.1029/2021EF002306.

Chou, C., J. C. H. Chiang, C.-W. Lan, C.-H. Chung, Y.-C. Liao, and C.-J. Lee. 2013. "Increase in the Range Between Wet and Dry Season Precipitation." *Nature Geoscience* 6, no. 4: 263–267. https://doi.org/10.1038/ngeo1744.

Chou, C., J. D. Neelin, C.-A. Chen, and J.-Y. Tu. 2009. "Evaluating the "Rich-Get-Richer" Mechanism in Tropical Precipitation Change Under Global Warming." *Journal of Climate* 22, no. 8: 1982–2005. https://doi.org/10.1175/2008JCLI2471.1.

Collow, A. B. M., M. A. Miller, and L. C. Trabachino. 2016. "Cloudiness Over the Amazon Rainforest: Meteorology and Thermodynamics." *Journal of Geophysical Research: Atmospheres* 121: 7990–8005. https://doi.org/10.1002/2016JD024848.

Costa, F. R. C., J. Schietti, S. C. Stark, and M. N. Smith. 2023. "The Other Side of Tropical Forest Drought: Do Shallow Water Table Regions of Amazonia Act as Large-Scale Hydrological Refugia From Drought?" *New Phytologist* 237: 714–733. https://doi.org/10.1111/nph.17914.

Csillik, O., M. Keller, M. Longo, et al. 2024. "A Large Net Carbon Loss Attributed to Anthropogenic and Natural Disturbances in the Amazon Arc of Deforestation." *Proceedings of the National Academy of Sciences* 121, no. 33: e2310157121. https://doi.org/10.1073/pnas.2310157121.

Dawson, T. E., and G. R. Goldsmith. 2018. "The Value of Wet Leaves." *New Phytologist* 219, no. 4: 1156–1169. https://doi.org/10.1111/nph.15307.

Donat, M. G., A. L. Lowry, L. V. Alexander, P. A. O'Gorman, and N. Maher. 2016. "More Extreme Precipitation in the World's Dry and Wet Regions." *Nature Climate Change* 6, no. 5: 508–513. https://doi.org/10.1038/nclimate2941.

Durieux, L., L. A. T. Machado, and H. Laurent. 2003. "The Impact of Deforestation on Cloud Cover Over the Amazon Arc of Deforestation." *Remote Sensing of Environment* 86, no. 1: 132–140. https://doi.org/10.1016/S0034-4257(03)00095-6.

Fan, Y., G. Miguez-Macho, E. G. Jobbágy, R. B. Jackson, and C. Otero-Casal. 2017. "Hydrologic Regulation of Plant Rooting Depth." *Proceedings of the National Academy of Sciences* 114, no. 40: 10572–10577. https://doi.org/10.1073/pnas.1712381114.

Fauset, S., M. O. Johnson, M. Gloor, et al. 2015. "Hyperdominance in Amazonian Forest Carbon Cycling." *Nature Communications* 6: 6857. https://doi.org/10.1038/ncomms7857.

Fricke, W. 2017. "Water Transport and Energy." *Plant, Cell & Environment* 40, no. 6: 977–994. https://doi.org/10.1111/pce.12848.

Friedl, M., and D. Sulla-Menashe. 2022. "MODIS/Terra+Aqua Land Cover Type Yearly L3 Global 500 m SIN Grid V061." https://doi.org/10.5067/MODIS/MCD12Q1.061.

Funk, C., P. Peterson, M. Landsfeld, et al. 2015. "The Climate Hazards Infrared Precipitation With Stations—A New Environmental Record for Monitoring Extremes." *Scientific Data* 2, no. 1: 150066. https://doi.org/10.1038/sdata.2015.66.

Gatti, L. V., L. S. Basso, J. B. Miller, et al. 2021. "Amazonia as a Carbon Source Linked to Deforestation and Climate Change." *Nature* 595, no. 7867: 388–393. https://doi.org/10.1038/s41586-021-03629-6.

Giglio, L., C. Justice, L. Boschetti, and D. Roy. 2021. "MODIS/Terra+Aqua Burned Area Monthly L3 Global 500 m SIN Grid V061." https://doi.org/10.5067/MODIS/MCD64A1.061.

Green, J. K., J. Berry, P. Ciais, Y. Zhang, and P. Gentine. 2020. "Amazon Rainforest Photosynthesis Increases in Response to Atmospheric Dryness." *Science Advances* 6, no. 47: eabb7232. https://doi.org/10.1126/sciadv.abb7232.

Grossiord, C., T. N. Buckley, L. A. Cernusak, et al. 2020. "Plant Responses to Rising Vapor Pressure Deficit." *New Phytologist* 226, no. 6: 1550–1566. https://doi.org/10.1111/nph.16485.

Guan, K., M. Pan, H. Li, et al. 2015. "Photosynthetic Seasonality of Global Tropical Forests Constrained by Hydroclimate." *Nature Geoscience* 8, no. 4: 284–289. https://doi.org/10.1038/ngeo2382.

Hammond, W. M., A. P. Williams, J. T. Abatzoglou, et al. 2022. "Global Field Observations of Tree Die-Off Reveal Hotter-Drought Fingerprint for Earth's Forests." *Nature Communications* 13, no. 1: 1761. https://doi.org/10.1038/s41467-022-29289-2.

Hansen, M. C., P. V. Potapov, R. Moore, et al. 2013. "High-Resolution Global Maps of 21st-Century Forest Cover Change." *Science* 342, no. 6160: 850–853. https://doi.org/10.1126/science.1244693.

Jung, M., C. Schwalm, M. Migliavacca, et al. 2020. "Scaling Carbon Fluxes From Eddy Covariance Sites to Globe: Synthesis and Evaluation of the FLUXCOM Approach." *Biogeosciences* 17, no. 5: 1343–1365. https://doi.org/10.5194/bg-17-1343-2020.

Khanna, J., D. Medvigy, S. Fueglistaler, and R. Walko. 2017. "Regional Dry-Season Climate Changes due to Three Decades of Amazonian Deforestation." *Nature Climate Change* 7, no. 3: 200–204. https://doi.org/10.1038/nclimate3226.

Konapala, G., A. K. Mishra, Y. Wada, and M. E. Mann. 2020. "Climate Change Will Affect Global Water Availability Through Compounding Changes in Seasonal Precipitation and Evaporation." *Nature Communications* 11, no. 1: 3044. https://doi.org/10.1038/s41467-020-16757-w.

Leite-Filho, A. T., B. S. Soares-Filho, J. L. Davis, G. M. Abrahão, and J. Börner. 2021. "Deforestation Reduces Rainfall and Agricultural Revenues in the Brazilian Amazon." *Nature Communications* 12, no. 1: 2591. https://doi.org/10.1038/s41467-021-22840-7.

Lian, X., C. Morfopoulos, and P. Gentine. 2024. "Water Deficit and Storm Disturbances Co-Regulate Amazon Rainforest Seasonality." *Science Advances* 10, no. 36: eadk5861. https://doi.org/10.1126/sciadv.adk5861.

Malavelle, F. F., J. M. Haywood, L. M. Mercado, et al. 2019. "Studying the Impact of Biomass Burning Aerosol Radiative and Climate Effects on the Amazon Rainforest Productivity With an Earth System Model." *Atmospheric Chemistry and Physics* 19: 1301–1326. https://doi.org/10.5194/acp-19-1301-2019.

Malhi, Y., D. Wood, T. R. Baker, et al. 2006. "The Regional Variation of Aboveground Live Biomass in Old-Growth Amazonian Forests." *Global Change Biology* 12: 1107–1138. https://doi.org/10.1111/j.1365-2486.2006.01120.x.

Marengo, J. A., C. A. Nobre, J. Tomasella, et al. 2008. "The Drought of Amazonia in 2005." *Journal of Climate* 21, no. 3: 495–516. https://doi.org/10.1175/2007JCLI1600.1.

Martens, B., D. G. Miralles, H. Lievens, et al. 2017. "GLEAM v3: Satellite-Based Land Evaporation and Root-Zone Soil Moisture." *Geoscientific Model Development* 10, no. 5: 1903–1925. https://doi.org/10.5194/gmd-10-1903-2017.

McAdam, S. A. M., and T. J. Brodribb. 2015. "The Evolution of Mechanisms Driving the Stomatal Response to Vapor Pressure Deficit." *Plant Physiology* 167: 833–843. https://doi.org/10.1104/pp.114.252940.

McDowell, N., C. D. Allen, K. Anderson-Teixeira, et al. 2018. "Drivers and Mechanisms of Tree Mortality in Moist Tropical Forests." *New Phytologist* 219: 851–869. https://doi.org/10.1111/nph.15027.

McDowell, N., W. T. Pockman, C. D. Allen, D. D. Breshears, N. Cobb, and T. Kolb. 2008. "Mechanisms of Plant Survival and Mortality During Drought: Why Do Some Plants Survive While Others Succumb to Drought?" *New Phytologist* 178, no. 4: 719–739. https://doi.org/10.1111/j.1469-8137.2008.02436.x.

Miguez-Macho, G., and Y. Fan. 2012. "The Role of Groundwater in the Amazon Water Cycle: 2. Influence on Seasonal Soil Moisture and Evapotranspiration." *Journal of Geophysical Research: Atmospheres* 117: D15114. https://doi.org/10.1029/2012JD017540.

Miralles, D. G., T. R. H. Holmes, R. A. M. De Jeu, J. H. Gash, A. G. C. A. Meesters, and A. J. Dolman. 2011. "Global Land-Surface Evaporation Estimated From Satellite-Based Observations." *Hydrology and Earth System Scences* 15, no. 2: 453–469. https://doi.org/10.5194/hess-15-453-2011.

Moser, P., M. F. Simon, M. B. de Medeiros, A. B. Gontijo, and F. R. C. Costa. 2019. "Interaction Between Extreme Weather Events and Mega-Dams Increases Tree Mortality and Alters Functional Status of Amazonian Forests." *Journal of Applied Ecology* 56: 2641–2651. https://doi.org/10.1111/1365-2664.13498.

Muñoz Sabater, J. 2019. *ERA5-Land Monthly Averaged Data From 1950 to Present*. Copernicus Climate Change Service (C3S) Climate Data Store (CDS). https://doi.org/10.24381/cds.68d2bb30.

Oliveira, R. S., C. B. Eller, F. d. V. Barros, M. Hirota, M. Brum, and P. Bittencourt. 2021. "Linking Plant Hydraulics and the Fast-Slow Continuum to Understand Resilience to Drought in Tropical Ecosystems." *New Phytologist* 230: 904–923. https://doi.org/10.1111/nph.17266.

Pan, Y., R. A. Birdsey, O. L. Phillips, et al. 2024. "The Enduring World Forest Carbon Sink." *Nature* 631, no. 8021: 563–569. https://doi.org/10.1038/s41586-024-07602-x.

Pavão, Q. S., P. G. Ribeiro, G. P. Maciel, et al. 2024. "Texture Prediction of Natural Soils in the Brazilian Amazon Through Proximal Sensors." *Geoderma Regional* 37: e00813. https://doi.org/10.1016/j.geodrs.2024.e00813.

Phillips, O. L., L. E. O. C. Aragão, S. L. Lewis, et al. 2009. "Drought Sensitivity of the Amazon Rainforest." *Science* 323, no. 5919: 1344–1347. https://doi.org/10.1126/science.1164033.

Qing, Y., S. Wang, B. C. Ancell, and Z.-L. Yang. 2022. "Accelerating Flash Droughts Induced by the Joint Influence of Soil Moisture Depletion and Atmospheric Aridity." *Nature Communications* 13, no. 1: 1139. https://doi.org/10.1038/s41467-022-28752-4.

Ren, S., X. Xu, G. Jia, A. Huang, and W. Ma. 2024. "Coherence of Recurring Fires and Land Use Change in South America." *Remote Sensing in Ecology and Conservation* 10: 628–641. https://doi.org/10.1002/rse2.390.

Restrepo-Coupe, N., K. S. Campos, L. F. Alves, et al. 2024. "Contrasting Carbon Cycle Responses to Dry (2015 El Niño) and Wet (2008 La Niña) Extreme Events at an Amazon Tropical Forest." *Agricultural and Forest Meteorology* 353: 110037. https://doi.org/10.1016/j.agrformet.2024.110037.

Restrepo-Coupe, N., H. R. da Rocha, L. R. Hutyra, et al. 2013. "What Drives the Seasonality of Photosynthesis Across the Amazon Basin? A Cross-Site Analysis of Eddy Flux Tower Measurements From the Brasil Flux Network." *Agricultural and Forest Meteorology* 182–183: 128–144. https://doi.org/10.1016/j.agrformet.2013.04.031.

Richards, J. H., E. M. Gora, C. Gutierrez, J. C. Burchfield, P. M. Bitzer, and S. P. Yanoviak. 2022. "Tropical Tree Species Differ in Damage and Mortality From Lightning." *Nature Plants* 8: 1007–1013. https://doi.org/10.1038/s41477-022-01230-x.

Romero, F., S. Cazzato, F. Walder, S. Vogelgsang, S. F. Bender, and M. G. A. van der Heijden. 2022. "Humidity and High Temperature Are Important for Predicting Fungal Disease Outbreaks Worldwide." *New Phytologist* 234: 1553–1556. https://doi.org/10.1111/nph.17340.

Rowland, L., A. C. L. da Costa, D. R. Galbraith, et al. 2015. "Death From Drought in Tropical Forests Is Triggered by Hydraulics Not Carbon Starvation." *Nature* 528: 119–122. https://doi.org/10.1038/nature15539.

Running, S., Q. Mu, and M. Zhao. 2015. "MOD17A2H MODIS/Terra Gross Primary Productivity 8-Day L4 Global 500 m SIN Grid V006." https://doi.org/10.5067/MODIS/MOD17A2H.006.

Running, S., Q. Mu, and M. Zhao. 2017. "MOD16A2 MODIS/Terra Net Evapotranspiration 8-Day L4 Global 500 m SIN Grid V006." https://doi.org/10.5067/MODIS/MOD16A2.006.

Ryu, Y.-H., and S.-K. Min. 2022. "Improving Wet and Dry Deposition of Aerosols in WRF-Chem: Updates to Below-Cloud Scavenging and Coarse-Particle Dry Deposition." *Journal of Advances in Modeling Earth Systems* 14: e2021MS002792. https://doi.org/10.1029/2021MS002792.

Seddon, A. W. R., M. Macias-Fauria, P. R. Long, D. Benz, and K. J. Willis. 2016. "Sensitivity of Global Terrestrial Ecosystems to Climate Variability." *Nature* 531, no. 7593: 229–232. https://doi.org/10.1038/nature16986.

Silva Junior, C. H. L., L. E. O. C. Aragão, L. O. Anderson, et al. 2020. "Persistent Collapse of Biomass in Amazonian Forest Edges Following Deforestation Leads to Unaccounted Carbon Losses." *Science Advances* 6, no. 40: eaaz8360. https://doi.org/10.1126/sciadv.aaz8360.

Slot, M., S. W. Rifai, C. E. Eze, and K. Winter. 2024. "The Stomatal Response to Vapor Pressure Deficit Drives the Apparent Temperature Response of Photosynthesis in Tropical Forests." *New Phytologist* 244: 1238–1249. https://doi.org/10.1111/nph.19806.

Stocker, B. D., S. J. Tumber-Dávila, A. G. Konings, M. C. Anderson, C. Hain, and R. B. Jackson. 2023. "Global Patterns of Water Storage in the Rooting Zones of Vegetation." *Nature Geoscience* 16: 250–256. https://doi.org/10.1038/s41561-023-01125-2.

Swinfield, T., O. T. Lewis, R. Bagchi, and R. P. Freckleton. 2012. "Consequences of Changing Rainfall for Fungal Pathogen-Induced Mortality in Tropical Tree Seedlings." *Ecology and Evolution* 2: 1408–1413. https://doi.org/10.1002/ece3.252.

Wang, X., M. Luo, F. Song, S. Wu, Y. D. Chen, and W. Zhang. 2024. "Precipitation Seasonality Amplifies as Earth Warms." *Geophysical Research Letters* 51: e2024GL109132. https://doi.org/10.1029/2024GL109132.

Wang, X.-Y., X. Li, J. Zhu, and C. A. S. Tanajura. 2018. "The Strengthening of Amazonian Precipitation During the Wet Season Driven by Tropical Sea Surface Temperature Forcing." *Environmental Research Letters* 13, no. 9: 094015. https://doi.org/10.1088/1748-9326/aadbb9.

Wentz, F. J., L. Ricciardulli, K. Hilburn, and C. Mears. 2007. "How Much More Rain Will Global Warming Bring?" *Science* 317, no. 5835: 233–235. https://doi.org/10.1126/science.1140746.

Wielicki, B. A., B. R. Barkstrom, E. F. Harrison, R. B. Lee, G. L. Smith, and J. E. Cooper. 1996. "Clouds and the Earth's Radiant Energy System (CERES): An Earth Observing System Experiment." *Bulletin of the American Meteorological Society* 77, no. 5: 853–868. https://doi.org/10.1175/1520-0477(1996)077<0853:CATERE>2.0.CO;2.

Xu, X., X. Zhang, W. J. Riley, et al. 2022. "Deforestation Triggering Irreversible Transition in Amazon Hydrological Cycle." *Environmental Research Letters* 17, no. 3: 034037. https://doi.org/10.1088/1748-9326/ac4c1d.

Yang, Y., R. J. Donohue, and T. R. McVicar. 2016. "Global Estimation of Effective Plant Rooting Depth: Implications for Hydrological Modeling." *Water Resources Research* 52: 8260–8276. https://doi.org/10.1002/2016WR019392.

Yang, Y., S. S. Saatchi, L. Xu, et al. 2018. "Post-Drought Decline of the Amazon Carbon Sink." *Nature Communications* 9: 3172. https://doi.org/10.1038/s41467-018-05668-6.

Yanoviak, S. P., E. M. Gora, P. M. Bitzer, et al. 2020. "Lightning Is a Major Cause of Large Tree Mortality in a Lowland Neotropical Forest." *New Phytologist* 225: 1936–1944. https://doi.org/10.1111/nph.16260.

Yuan, W., Y. Zheng, S. Piao, et al. 2019. "Increased Atmospheric Vapor Pressure Deficit Reduces Global Vegetation Growth." *Science Advances* 5, no. 8: eaax1396. https://doi.org/10.1126/sciadv.aax1396.

Zhang, Y., D. Kong, R. Gan, et al. 2019. "Coupled Estimation of 500 m and 8-Day Resolution Global Evapotranspiration and Gross Primary Production in 2002-2017." *Remote Sensing of Environment* 222: 165–182. https://doi.org/10.1016/j.rse.2018.12.031.

Zhang, Y., C. Li, F. H. S. Chiew, et al. 2023. "Southern Hemisphere Dominates Recent Decline in Global Water Availability." *Science* 382, no. 6670: 579–584. https://doi.org/10.1126/science.adh0716.

Zhang, Y., X. Xiao, X. Wu, et al. 2017. "A Global Moderate Resolution Dataset of Gross Primary Production of Vegetation for 2000-2016." *Scientific Data* 4, no. 1: 170165. https://doi.org/10.1038/sdata.2017.165.

Supporting Information

Additional supporting information can be found online in the Supporting Information section. **Data S1:** gcb70422-sup-0001-supinfo.pdf.